Decay-Induced Changes in the Physical and Mechanical Properties of First Year Ice.

Johnston, Michelle; Frederking, Robert; Timco, Garry

Publisher’s version / Version de l'éditeur:

Proceedings 16th International Conference on Port and Ocean Engineering under Arctic Conditions, POAC'01, pp. 1395-1404, 2001-08-12

POAC '01
Ottawa, Canada

Proceedings of the 16th International Conference on
Port and Ocean Engineering under Arctic Conditions
POAC'01
August 12-17, 2001
Ottawa, Ontario, Canada

DECAY-INDUCED CHANGES IN THE PHYSICAL AND MECHANICAL PROPERTIES OF FIRST YEAR ICE

M. Johnston, R. Frederking and G. Timco
Canadian Hydraulics Centre
National Research Council
Ottawa, Ontario K1A 0R6 Canada

ABSTRACT

This paper describes the results and analysis of one season of measurements of decayed first year sea ice in the central Canadian Arctic. The study was conducted from 21 May to 19 July 2000 during which time the mean air temperature steadily increased from –15°C to a maximum of +7.5°C. The ice was 1.20 m thick when the program began on 21 May and had decreased to 0.83 m thick by 19 July. On average, the ice ablated at a rate of about 23 mm/day during the program. Initially, the average salinity throughout the full thickness of ice was 5.5 ‰. By 19 July measurements showed that the bulk salinity of the ice had decreased to less than 0.5 ‰. The upper and lower surfaces of the ice began to desalinate before the bulk layer of ice. One of the main components of the study was to measure the *in situ* confined compressive strength of the ice with a borehole jack assembly; 110 borehole jack tests were conducted from 21 May to 19 July. Over the nine-week period, the *in situ* strength of the ice decreased from 12 to 3 MPa. Measurements showed that the ice maintained a strength of 3 MPa during the last three weeks of the study. The ice continued to ablate during that time. Most of the decrease in ice strength resulted from changes in the physical properties of the ice.

INTRODUCTION

Remote sensing is a tool that is widely used to characterize ice conditions by organizations such as Canadian Ice Service (CIS) and the United States National Ice Centre (NIC). As a result, a considerable amount of effort has been devoted to relating the ice surface properties to the microwave signature of the ice in remotely acquired imagery. That has been the primary objective of projects such as the Seasonal Sea Ice Monitoring and Modelling Site (SIMMS) and the Collaborative-Interdisciplinary Cryospheric Experiment (C-ICE), for instance see LeDrew and Barber (1994). Those studies focused upon the ice surface, since incident microwave energy penetrates only the surface layer of saline, first year sea ice.

Having identified the problem of relating the ice surface properties to the microwave signature of the ice, the next formidable question arises: "How does the ice signature relate to the bulk physical properties of the ice?" Answering both those questions would directly benefit the end users of remotely sensed data products from CIS and NIC. The spring transition of the ice is a logical place to begin examining the relation between the surface and bulk physical properties of the ice and the ice microwave signature. This paper documents changes in the ice properties that occur (both externally and internally) during the decay process.

BACKGROUND

Ice property measurements are usually conducted before mid-May (Sinha, 1986; Prowse et al., 1988; Sinha, 1990; and Masterson et al., 1997; Masterson and Yockey, 2000; Spencer et al., 2001). In winter and early spring, it is relatively easy to access the ice and measurement techniques are relatively straightforward. Once the air temperatures and solar radiation increase, the physical properties of the snow and ice quickly begin to change. In spring, field measurements that require extraction of ice cores from the parent ice sheet become exceedingly difficult. That is because when air temperatures are warm, significant changes take place in the ice the moment that the core is removed from the ice sheet. The absence of data on the properties of deteriorating first year sea ice led to the development of a field program in which the basic physical properties of the ice were measured during the spring transition of first year sea ice in the Canadian Arctic Archipelago.

This paper provides a summary of the data acquired over a nine-week field program that extended from 21 May to 19 July 2000. The analysis was based upon physical property measurements of the snow and ice. Measured surface properties included the snow depth, snow density, and air temperature. Bulk ice property measurements included the ice freeboard, ice thickness, ice temperature, ice salinity and the *in situ* confined, compressive strength of the ice. The reader is referred to Johnston et al. (2001) for a complete description of the program and data analysis.

FIELD PROGRAM

In early May, the measurement site was selected as landfast ice in McDougall Sound, 5 km east of the base camp on Truro Island (75°14.4'N, 97°09.3'W) Nunavut. The selected site consisted of sufficiently level first year sea ice, with no evidence of roughness or pressure ridging, and a 0.18 m thick snow cover. Figure 1 shows the sea ice measurement site in late May and late June. Snow and ice property measurements were conducted over a 900 m^2 area of ice from 21 May to 1 July. Each week, a field party visited the same area of ice by snowmobile and performed the measurements at stations selected about 5 m apart. As the decay season advanced, site visits were made twice per week.

(a) late May, courtesy of K. Wilson (b) 21 June, courtesy of D. Bradley

Figure 1 First year sea ice measurement site

A motor driven, fibre-glass corer was used to make three boreholes in the ice (0.15 m diameter), each about 1.5 to 2.0 m apart. The ice thickness, freeboard and snow depths were measured at each borehole. The ice core from the first borehole was used to profile the ice temperature. A thermal probe was inserted into small holes made in the core at depth intervals of 0.15 m. The second core was used for salinity measurements. Discs (20 mm thick) were cut from the core at 0.15 m intervals. The sections were cut as quickly as possible to minimize brine drainage. Samples were promptly bagged and left to melt at room temperature. The salinity of the melt water was later measured with an optical refractometer. The core from the third borehole was not used for property measurements.

The ice *in situ* borehole strength, the *in situ* confined compressive strength (Masterson, 1996), was measured at each of the three holes using a borehole jack assembly. The borehole jack consists of a high-strength stainless steel hydraulic cylinder with a laterally acting piston and two indentor plates, curved to match the wall of the borehole. Once activated, the piston inside the body of the jack applies hydraulic pressure to the front and back indentor plates. The oil pressure and displacement of the indentor plate were recorded by an external digital acquisition system.

Borehole jack tests for each hole were conducted at depth intervals of 0.30 m. Typically, four borehole jack tests were performed at each hole before the bottom of the ice was reached. During the tests, the indentor plate was extended continuously until the limit of the stroke ram was reached (50 mm total diametrical displacement) or concern was expressed about overloading the jack. At that point the indentor plate was retracted fully, the jack was rotated 90° and lowered to the next test depth.

ICE PROPERTY AND *IN SITU* STRENGTH MEASUREMENTS

As the decay season progressed, the ice began to develop an undulating surface. Melt ponds covered some areas of ice, while other regions began to develop a hummocked appearance (elevated, white, porous ice, Figure 1). Since it became exceedingly difficult to locate level ice later in the program, measurements were made in ponded ice and hummocked ice as a matter of course. The following discussion is based upon the average properties measured at each station (two to four boreholes) at each sampling site.

Air Temperature and Ice Temperature

Figure 2 shows the mean air temperature, ice temperature and the snow and ice thickness versus sample date. The mean air temperature (courtesy of Atmospheric Environment Service) was –15°C when the ice site was first visited on 21 May (Julian Day (JD) 142). The highest temperature during the field program was +7.5°C on 7 July (JD189). The mean air temperature first rose above zero on 10 June (JD162), after which it continued to increase with intermittent cold spells. The ice temperature near the surface of the ice also continued to increase. Open circles were used to denote the ice temperature measurements after JD163, since those measurements were less reliable than the earlier measurements due to increasing air temperatures (see Johnston and Frederking, 2001).

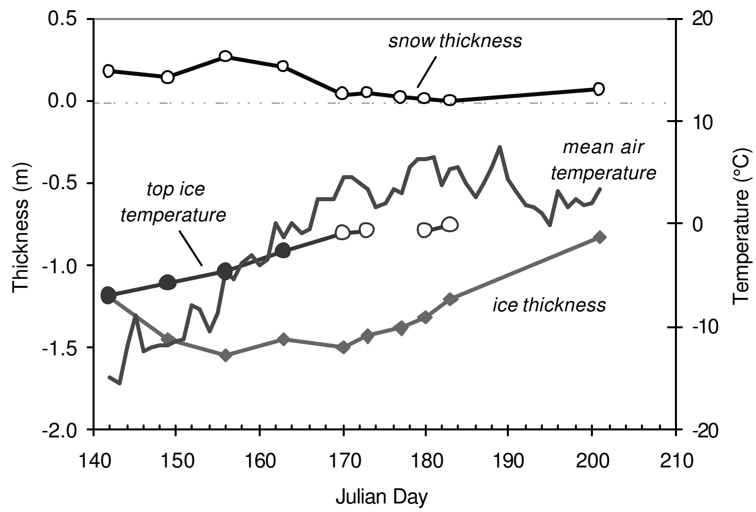

Figure 2 Measured temperatures and snow and ice thickness

Snow and Ice Thickness

Figure 2 shows that the 0.18 m thick snow cover melted little during the first week. On 4 June (JD156) both the snow cover and ice thickness reached their maximum extent (0.27 m, and 1.55 m respectively). By 18 June (JD170), the 270 mm snow cover rapidly decreased to just 40 mm. The first decrease in ice thickness occurred on 18 June (JD170) indicating that, once the ice surface was exposed, the ice began to ablate. After 18 June, ice ablation continued (at relatively constant rate of 23 mm per day) until the last ice thickness measurement of 0.83 m was taken on 19 July (JD201).

Ice Salinity

Figure 3 shows representative salinity profiles for five of the sampling dates. The ice salinity profiles remained relatively stable until 18 June (JD170), when the surface salinity decreased by 6 ‰ and there was a 1 ‰ decrease in salinity at the bottom of the ice. The decrease in the ice surface salinity between JD142 and JD149 is believed to be inaccurate. It was on 18 June that the ice first began to decrease in thickness. On 19 July (JD201) measurements showed that the ice had a salinity of less than 0.5 ‰ throughout its full thickness of 0.83 m. Due to the substantial amount of brine drainage during the later stages of the experiment, the 0.5 ‰ salinity profile that was measured on JD201 would have been significantly lower than the *in situ* ice salinity.

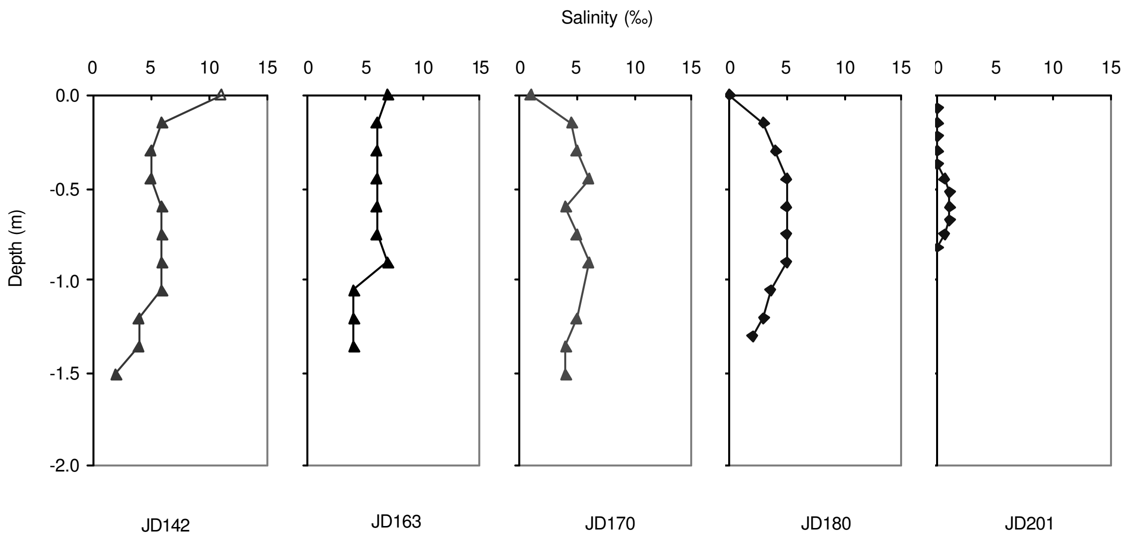

Figure 3 Salinity profiles during the study, 21 May (JD142) to 19 July (JD201)

Borehole Strength

More than 100 borehole jack tests were conducted during the study. The borehole jack data from each test were used to generate three plots, (a) *in situ* ice pressure versus time, (b) indentor penetration (one half the displacement of the two end platens) versus time and (c) *in situ* ice pressure versus indentor penetration. Indentor penetration is defined as one-half the diametrical displacement of the borehole jack. Figure 4 is a schematic that shows the *in situ* pressure (σ) and indentor penetration (δ) as a function of time. The figure shows that, as the borehole jack is extended, the *in situ* ice pressure increases until a peak pressure is attained, σ_M. Typically, after σ_M has been reached, the pressure drops and then stabilizes.

A standardized approach was needed to compare results from the 110 borehole jack tests. Since σ_M was not always captured during the tests (due to the limit of the stroke ram and/or concern about overloading the jack), the common factor used to compare all tests was defined as σ_{3mm}, the *in situ* pressure at an indentor penetration of 3 mm. Figure 4 shows a comparison between σ_M and σ_{3mm}. During the early borehole jack tests, the ice was sufficiently cold so that σ_M occurred after a penetration of 3 mm (δ_{3mm}). As the ice decayed, its temperature increased and the ice presented less resistance to the indentor. As a result, σ_M was reached more quickly and there was very little (if any) difference between σ_M and σ_{3mm}, as discussed subsequently.

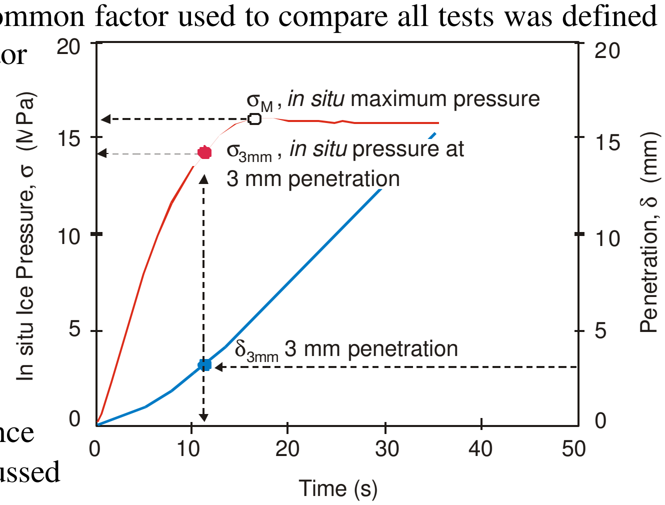

Figure 4 Schematic of σ for arbitrary test

Figure 5 shows the ice pressure (σ) and indentor penetration (δ) versus time curves for the surface layer of ice for two different borehole jack tests. First shown is the *in situ* borehole strength of cold ice at the beginning of the study (–7°C on 21 May, JD142). In comparison, Figure 5-b shows the *in situ* borehole strength of warm ice at the end of the study (–1.8°C on 19 July, JD201). The two borehole jack tests show that cold first year ice had a σ_{3mm} of 14.8 MPa whereas warm, decayed ice had a σ_{3mm} of only 1.9 MPa. The overall shape of the curves is considerably different for the two tests. For cold ice, the pressure continued to increase until the borehole jack was retracted at 19 s (Figure 5-a) whereas tests in the decayed ice showed that the ice pressure reached a plateau after about 5 s, and remained at that level until the jack was retracted (at about 25 s, Figure 5-b).

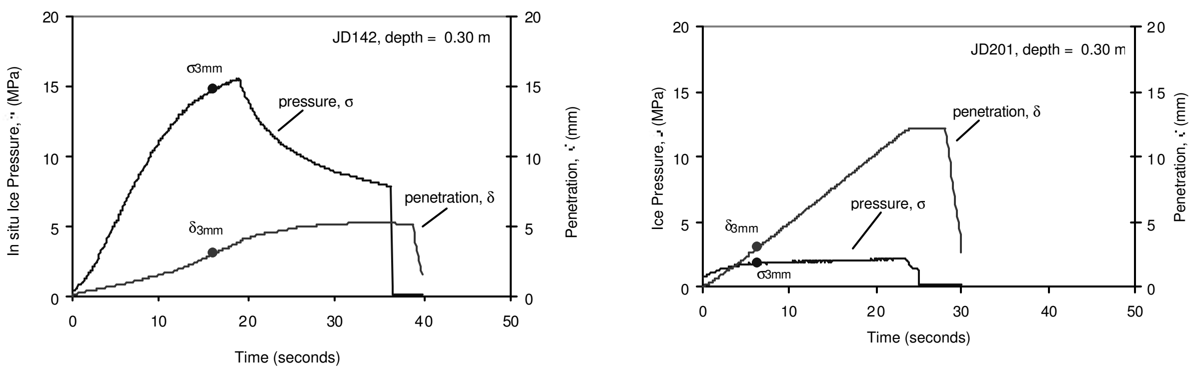

(a) 21 May (JD142) **(b) 19 July (JD201)**

Figure 5 Two examples of σ and δ in upper layer of ice, d = 0.30 m

Borehole Jack Data as a function of Ice Depth and Time

Figure 6 shows σ_{3mm} for ice depths of 0.3 m and 1.2 m as a function of the day on which the tests were conducted. The plots include the borehole jack measurements from each hole (crossed data symbol) as well as the average of the individual *in situ* borehole strengths (oversized symbol). Figure 6-a shows that σ_{3mm} decreased by about 1 MPa per week during the first four weeks (JD142 to JD163, 21 May to 11 June). A much larger decrease of 4.5 MPa in σ_{3mm} occurred during the fourth week (JD163 to JD170, 11 June to 18 June). After that, there was a gradual reduction in σ_{3mm} until the last tests were conducted on JD201 (19 July). Note that the strength of the surface layer changed only 0.6 MPa during the last three weeks of the study (JD183 to JD201, July 1 to July 19). Most of the change in ice strength at this depth occurred between the third and sixth weeks. The change in σ_{3mm} that characterized the ice from JD156 to JD183 was used to calculate the average rate of ice decay (0.5 MPa/day). Measurements of σ_{3mm} indicate that the standard deviation of tests conducted on the same day ranged from 0.2 to 1.3 MPa when sampled at the same depth.

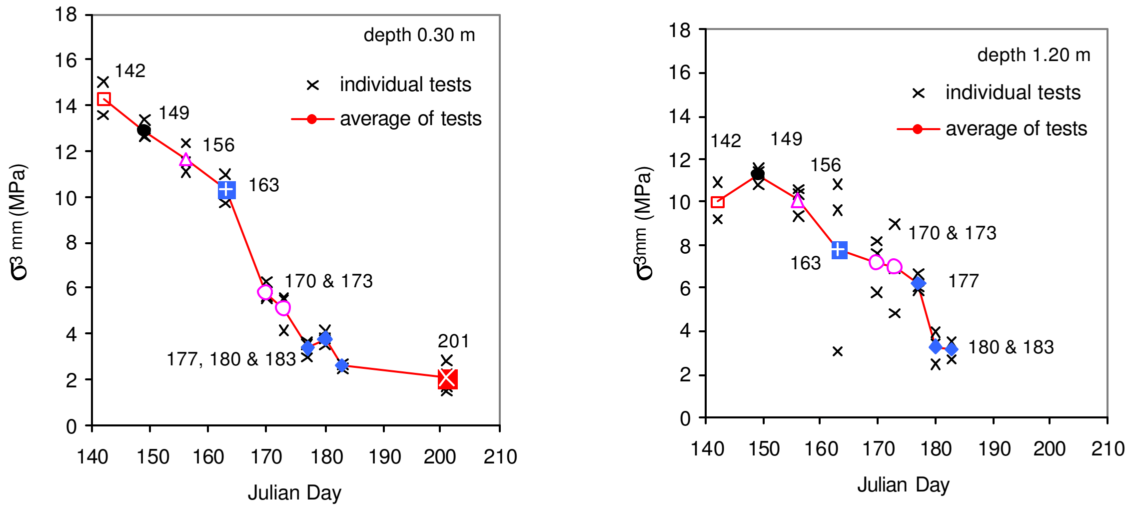

(a) depth 0.30 m **(d) depth 1.20 m**

Figure 6 Seasonal changes in the *in situ* borehole strength, σ_{3mm}

The most significant decrease in σ_{3mm} in the bottom ice occurred from 25 to 28 June (JD177 to JD180, Figure 6-b). Within the course of three days, σ_{3mm} had decreased by 3.0 MPa at the 1.2 m ice depth. The ice decay rate from JD156 to JD183 was 0.4 MPa/day. Unlike the borehole jack tests conducted at the other depths, tests from a depth of 1.2 m show considerable scatter in σ_{3mm} between 11 to 21 June (JD163 to JD173). Since only those tests showed scatter in σ_{3mm}, the variation was probably an artifact introduced during testing.

Relation between Physical Properties and Borehole Strength

Figure 7 illustrates the relation between the average *in situ* borehole strength ($\underline{\sigma}_{3mm}$, averaged over the full thickness of the ice) and changes in physical properties of the ice. The warm air/ice temperatures after 28 June (JD180) made it difficult to accurately measure the ice salinity due to accelerated brine drainage. However the late-season salinity measurements indicate that the ice became nearly fresh during the late stages of ice decay. Ice temperature measurements after 11 June (JD163) are subject to uncertainty, for previously discussed reasons.

The first notable decrease in $\underline{\sigma}_{3mm}$ occurred between JD156 and JD163. The *in situ* ice strength, $\underline{\sigma}_{3mm}$, was 11 MPa on 4 June (JD156) and had decreased to 9 MPa by 11 June (JD163). The decrease in $\underline{\sigma}_{3mm}$ continued until 1 July (JD183), when the ice reached a plateau of 3 MPa. The average *in situ* ice strength remained at the 3 MPa plateau until the last measurement was taken on 19 July (JD201).

Although $\underline{\sigma}_{3mm}$ began to decrease on 4 June (JD156), the ice thickness did not change appreciably (from 1.5 m) until two weeks later (18 June, JD170). Between 18 June (JD170) and 19 July (JD201) the ice thickness decreased by 0.67 m. Ice ablation continued until the end of the study; three weeks after $\underline{\sigma}_{3mm}$ reached a plateau. Despite the different intervals over which $\underline{\sigma}_{3mm}$ and the ice thickness decreased, both occurred at uniform rates. The rate of decrease of $\underline{\sigma}_{3mm}$ was 0.30 MPa/day (until 1 July, JD180) and the ice thickness decreased by 23 mm/day (until the last measurement was obtained on 19 July, JD201).

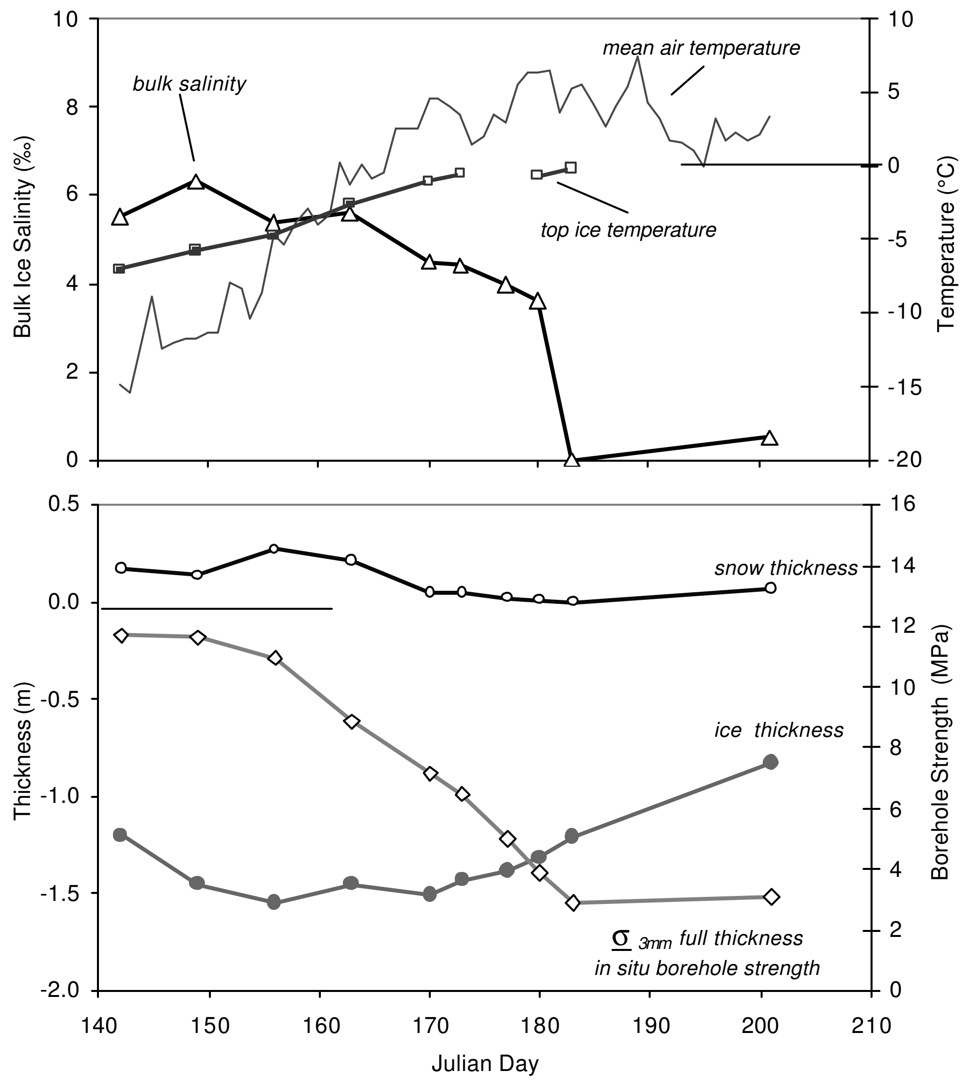

Figure 7 Relation between physical property measurements and $\underline{\sigma}_{3mm}$

What were the external factors that resulted in first, a decrease in ice strength and second, a decrease in ice thickness? Figure 7 shows that the air temperature and ice temperature obviously influenced the onset of ice decay. On 10 June (JD162) the mean air temperatures rose above zero for the first time that season and the snow cover rapidly melted. The first signs of decreased ice strength coincided with the decrease in snow cover and increase in air/ice temperatures. After the insulating layer of snow melted, the ice was exposed to the warm air temperatures and the ice rapidly desalinated and began to ablate. The ice strength continued to decrease until it reached a plateau. The stabilization in ice strength coincided with the point at which the ice had desalinated almost completely.

SUMMARY AND CONCLUSIONS

The nine-week study was conducted from 21 May to 19 July 2000. Surface property measurements included the air temperature, snow depth and snow density. The measured bulk physical properties of the ice included freeboard, thickness, temperature, salinity and *in situ* confined compressive strength of the ice.

Mean air temperatures increased steadily during the study from –15°C to a maximum of +7.5°C, near the end of the study. Physical property measurements began on 21 May at which time the ice thickness was 1.20 m. The ice continued to increase in thickness until 4 June, when a maximum thickness of 1.55 m was attained. The ice remained about 1.5 m thick until two weeks later, 18 June, when it began to ablate. As ablation continued, the ice developed an undulating surface. When the last measurements were conducted on 19 July the ice was only 0.83 m thick. The 0.67 m of ice that ablated during the study did so at a relatively constant rate of 23 mm/day.

Salinity measurements showed that the surface and underside of the ice began to desalinate at about the same time. During the decay process, the ice developed a salinity profile distinctly different from the "C" shaped profile that typically characterizes cold, first year sea ice (higher salinity in the upper and lower parts of the ice sheet, see Nakawo and Sinha, 1981). Rather, the upper and lower surfaces of the ice began to desalinate before the bulk layer of ice, causing a reversed "C" shaped salinity profile. The ice maintained a reversed "C" shaped profile until the last salinity measurements were made on 19 July, at which point the entire ice thickness was nearly devoid of brine (ice salinity of 0.5 ‰).

The *in situ* confined compressive strength of the ice (σ) was measured in 110 borehole jack tests. Once (or twice) per week, the tests were conducted in a number of boreholes, at depth intervals of 0.30 m. Typically, four borehole jack tests were performed in each hole. There was good repeatability of the data; measurements show that the standard deviation of tests conducted on the same day ranged from 0.2 to 1.3 MPa when sampled at the same depth. All strength profiles showed that σ decreased as the decay season progressed.

The borehole strengths from each test were compared using 3 mm indentor penetration as a common factor (σ_{3mm}). During the first three weeks of the study, σ_{3mm} in the surface layer of ice (depth 0.30 m) was about 2 to 4 MPa higher than in the bottom layer of ice. By 18 June, however, the ice surface had deteriorated to such an extent that σ_{3mm} in the bottom ice was larger than near the ice surface. After 25 June, σ_{3mm} of the upper and lower ice surfaces were quite similar.

Over the nine-week period, the average full-thickness strength of the ice ($\underline{\sigma}_{3mm}$ obtained by depth-averaging individual borehole strengths) decreased from 12 MPa to 3 MPa. Most of the decrease in $\underline{\sigma}_{3mm}$ resulted from changes in the physical properties of the ice. About 20% (2 MPa) of the decrease was caused by the different stress rates of the borehole jack tests (Johnston and Frederking, 2001). The first significant decrease in $\underline{\sigma}_{3mm}$ (2 MPa) occurred from 4 to 11 June. The $\underline{\sigma}_{3mm}$ decreased by a relatively constant rate of about 0.30 MPa/day until 1 July when it reached 3 MPa. Once $\underline{\sigma}_{3mm}$ had decreased to 3 MPa, it remained at that level until the end of the study (three weeks later). Results showed that while the ice started to ablate nearly two weeks after the ice strength began to decrease, ice ablation continued until the end of the study (three weeks after $\underline{\sigma}_{3mm}$ had reached the 3 MPa plateau).

ACKNOWLEDGEMENTS

Funding for the Canadian Hydraulics Centre (CHC) participation in the program was provided by Transport Canada and it is gratefully acknowledged. Canadian Ice Service (CIS) performed the required measurements. The field project was conducted under the auspices of the Collaborative-Interdisciplinary Cryospheric Experiment (C-ICE'00) of the University of Manitoba. Polar Continental Shelf Project (PCSP) provided field support.

REFERENCES

LeDrew, E. and D. Barber (1994) "The SIMMS Program: A Study of Change and Variability within the Marine Cryosphere", Arctic, Vol. 47, No. 3, pp. 256 – 264.

Johnston, M., Frederking, R. and G. Timco (2001) Seasonal Decay of First Year Sea Ice, Technical Report HYD-TR-058, April 2001, Canadian Hydraulics Centre, 24 pp.

Nakawo, M. and N.K. Sinha (1981) "Growth Rate and Salinity Profile of First Year Sea Ice in the High Arctic", J. Glac., Vol. 27, No. 96, pp. 315 – 330.

Masterson, D.M., Graham, W.P., Jones, S.J. and G.R. Childs (1997) "A Comparison of Uniaxial and Borehole Jack Tests at Fort Providence Ice Crossing, 1995", Can. Geotech. J., Vol. 34, pp. 471 – 475.

Masterson, D.M. (1996) "Interpretation of *In Situ* Borehole Ice Strength Measurements Tests" Canadian Journal of Civil Engineering, Vol. 23, No. 1, pp. 165 – 179.

Masterson, D.M. and D.E. Yockey (2000) "Field Strength Properties of a Flooded Sea Ice Road", 10th Int. Offshore and Polar Engineering Conference (ISOPE'00), Seattle, Washington, 28 May– 2 June 2000.

Spencer, P.A., Masterson, D.M. and K.E. Yockey (2001) "Floating Sea ice Road Strength from Borehole Jack Data: Northstar 2000", 16th Intl. Conference on Port and Ocean Engineering under Arctic Conditions (POAC'01), Ottawa, Canada, 12 – 17 August 2001, in print.

Prowse, T.D, Demuth, M.N. and C.R. Onclin (1988) "Using the Borehole Jack to Determine Changes in River Ice Strength", Proc. of Workshop on Hydraulics of River Ice/Ice Jams, Winnipeg, June 1988, pp. 283 – 301.

Sinha, N.K. (1986) "The Borehole Jack, Is It a Useful Arctic Tool?", Proc. Fifth Int. Offshore Mech. and Arctic Eng. Sym. (OMAE'86), Tokyo, Japan, 13 – 17 April, 1986, Vol. IV, pp. 328 - 335.

Sinha, N.K. (1990) "Ice Cover Strength Decay using Borehole Indentor", Proc. Tenth Int. Sym. on Ice (IAHR), Espoo, Finland, Vol. 2, pp. 735 – 744.